

DESIGN OF HIGHLY ISOLATED UWB MIMO ANTENNA USING STUBS BETWEEN GROUND PLANES

Gosangi Lilly Grace
Department of ECE
RVR&JC College of Engineering
Guntur,India
gracelight0333@gmail.com

Garikapati Hima Bindu
Department of ECE
RVR&JC College of Engineering
Guntur,India
himabindugarikapati215@gmail.com

Anusuri Sonu Sampath
Department of ECE
RVR&JC College of Engineering
Guntur,India
sampathanusuri03@gmail.com

Garnepudi Jaswanth
Department of ECE
RVR&JC College of Engineering
Guntur,India
jaswanthgarnepudi2003@gmail.com

ABSTRACT

This study introduces an in-depth analysis and evaluation of a novel High-Isolation Ultra-Wideband (UWB) Multiple Input Multiple Output (MIMO) antenna design featuring the integration of Stubs between ground planes. The objective is to develop an antenna system capable of achieving high isolation between closely spaced antenna elements for MIMO applications while maintaining a wide operating bandwidth. The proposed antenna is composed of four slot antenna elements with a common rhombic slot, each fed by a microstrip-fed line to greatly reduce the overall size of the antenna. It has a compact size of (34 x 34 x 1.6 mm³). The wide frequency range of Ultra-wide band lies in the range of 3.1 to 10.6 GHz and wide channel bandwidths of 500 MHz. The combination of ultra-wideband multiple-input and multiple-output (UWB MIMO) technology has high transmission rate, good communication quality and large channel capacity. Investigation will be done with respect to correlation parameter coefficients, radiation characteristics, efficiency, realized gain and the active reflection coefficient. In essence, the Highly Isolated MIMO Antenna marks a significant stride in antenna technology and in the field of wireless communication. CST (Computer Simulation Technology) is used to design the proposed antenna.

Keywords-Antenna, Isolation, UWB, MIMO, Stubs, S-Parameter Results.

1. INTRODUCTION

As wireless communication advances, we demand better quality and faster speeds. To meet these needs, we've introduced MIMO technology, which uses multiple antennas on both ends of the communication link. This allows us to increase system capacity through multiplexing and enhance reliability using diversity techniques. However to ensure MIMO works effectively, we must reduce correlation between the

antennas. Therefore, Combining Ultra-Wideband (UWB) technology with MIMO allows for the simultaneous transmission of multiple paths without the need to increase antenna radiation power. This results in a significant improvement in the transmission distance of UWB systems. UWB MIMO technology has garnered considerable attention due to its ability to achieve high transmission rates, excellent communication quality and substantial channel capacity. When designing UWB

MIMO antennas, there are two main ground plane structures: separate ground planes and shared ground planes. It's generally found that using separate ground planes results in better isolation between antenna elements compared to shared ground planes. To reduce coupling between the antenna elements, slotted rectangular parasitic stubs are added to the ground plane. These stubs are strategically placed between the ground planes of the antenna elements to achieve the high isolation and a wide operating frequency band. By concentrating most of the current on the loaded branches when connecting the ground planes the mutual coupling between the antenna elements is reduced. Through experimental measurements, it is observed that the isolation remains consistently above 20.1 dB across the frequency band of 3.1–10.6 GHz. Additionally, metrics such as the envelope correlation coefficient (ECC), mean effective gain (MEG), and channel capacity loss (CCL) all meet the requirements for practical applications. The two-port MIMO antenna design is expanded into a four-port MIMO antenna configuration, with adjacent antenna elements positioned orthogonally. Similarly the stubs are utilized between the ground planes of the antenna elements and arranged in opposite directions. This allows the antenna structure to share the same ground plane. Simulation results demonstrate that the antenna maintains isolation above 20.1 dB across the frequency range of 3.1–10.6 GHz. This confirms that the isolation improvement method employed in the four-port UWB MIMO antenna. Moreover, the smaller size of the antenna ($34 \times 34 \times 1.6 \text{ mm}^3$) facilitates easier integration with modern wireless communication equipment.

2. DIMENSION SPECIFICATIONS

Certain design parameters of the UWB antenna can be determined using the wavelength (λ) corresponding to the low frequency of the antenna, which is typically 3.7 GHz. The length (L_p) of the rectangular radiation patch should fall within a specific range, where it is at least one-tenth of the wavelength ($\lambda/10$) but no more than one-fifth of the wavelength ($\lambda/5$). The effective length of the antenna, which is the combination of the length of the rectangular radiating patch (L_p) and the length of the microstrip feeder (L_f), approximately equals one-fifth of the wavelength ($\lambda/5$). The length of the feed gap, which is the difference between the length of the microstrip feed line (L_f) and the length of a portion of the ground plane (L_g), should be within 0.02λ to 0.04λ . The thickness of the dielectric substrate (H) can be approximated as 0.02 times the wavelength (0.02λ).

3. DESIGN OF UWB MIMO ANTENNA

We've developed an enhanced UWB antenna using a rectangular radiating patch and a microstrip feeder. This antenna is constructed on a dielectric substrate made of FR4 material.

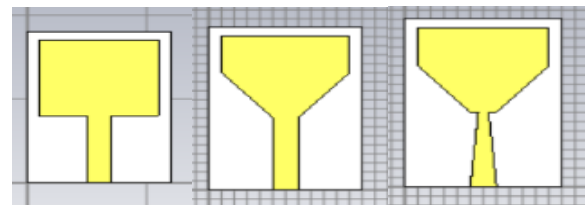


Fig 1. Schematic diagram of UWB antenna structure a) rectangular radiating patch b) cutting off the rectangular grooves of the patch c) cutting off the feed line.

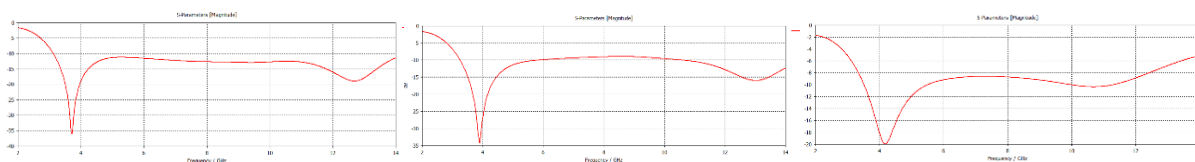


Fig 2. Simulated results (S11) of structures a, b and c.

4. DESIGN STRUCTURE OF CONNECTED GROUND PLANES

The antennas are spaced 4 mm apart on this substrate. This distance is important because it affects how signals received by each antenna correlate with each other. Ideally, you want some separation to capture

different signal paths, which improves performance. Overall, this setup forms a wideband MIMO antenna structure, suitable for applications where high-speed data transfer and reliable communication are needed.

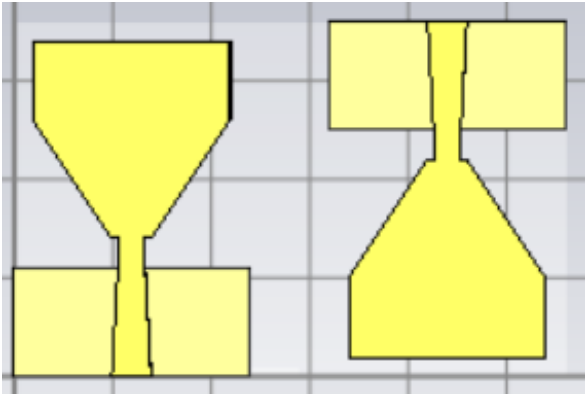
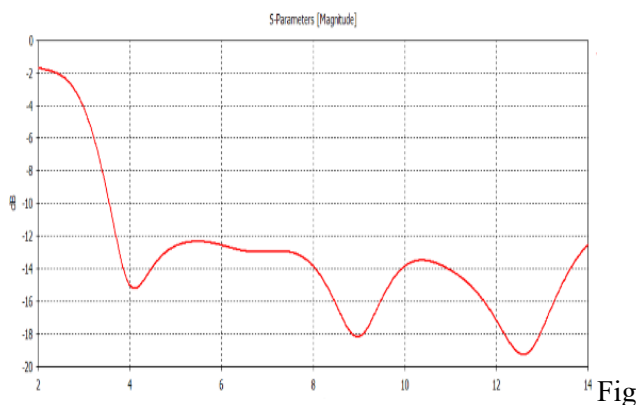
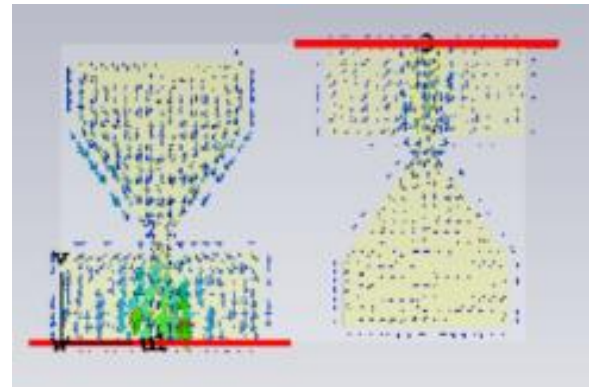


Fig 3. Schematic Diagram of UWB MIMO Antenna Structure without decoupling structure.



4. S-parameter wave form.



Fig

5. Surface Current Distribution of antenna

The simulation results indicate that when the left port of the antenna is connected to the signal source and the right port is linked to a 50 Ω load, there's significant current transfer to the right antenna element. This coupling of current reduces the independence between the antenna elements. It's noted that because the two ground planes of the antenna elements aren't connected, there's no coupling of ground current. The primary reason for this coupling is spatial, meaning it arises due to the proximity of the antenna elements. Despite this coupling, the isolation between the antenna elements remains above 13.6 dB within the 3.2–14 GHz frequency band. However, this level of isolation is deemed insufficient for MIMO systems. In practical scenarios, MIMO antennas typically need to share a common ground plane with the system they are part of. As the antenna elements in this configuration do not share a ground plane, it's unsuitable for wireless communication systems. Therefore, to address this issue, it's suggested that the antenna elements should be connected to the ground. This modification allows for better performance and suitability of the MIMO antenna for wireless communication applications.

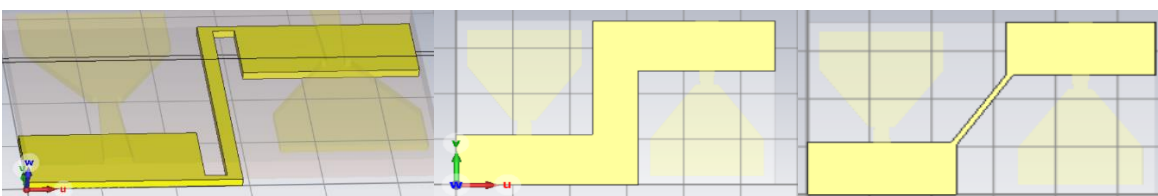


Fig 6. Schematic diagram of connection structures of two ground planes.

The diagram in Figure 6 illustrates how three ground planes are connected. To enhance the performance of an Ultra-Wideband (UWB) Multiple-Input Multiple-Output (MIMO) antenna. The return loss for A1 and A2 connection structures is higher than -10 dB within certain frequency ranges, indicating poor performance in those bands and hindering normal operation. Additionally, the isolation between antenna elements in the passband is relatively low for A1 and A2, measured at 12.9 dB and 16.2 dB respectively. On

the other hand, A3 connection structure shows promising characteristics: It maintains good impedance matching across a wider frequency range of 1.9–14 GHz and achieves isolation higher than 18.4 dB. This suggests that incorporating a stub between ground planes effectively enhances isolation between antenna elements and expands the working frequency band. As the coverage area of these connection stubs increases for A1 and A2, the isolation within the passband improves while the S11 (return loss) result remains relatively unchanged.

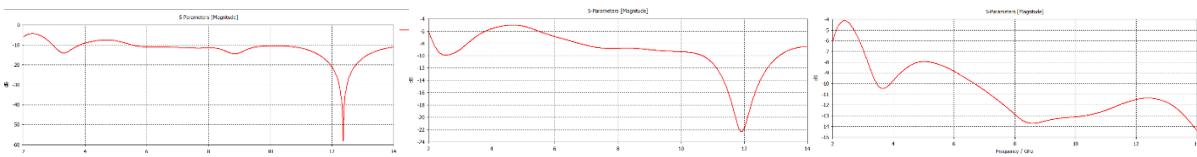


Fig 7. S-parameter simulation results of three connection structures.

5. DESIGN OF FOUR-PORT UWB MIMO ANTENNA WITHOUT STUBS

Based on the decoupling principle used in the design of the two-port Ultra-Wideband (UWB) Multiple-Input Multiple-Output (MIMO) antenna, adjacent antenna elements are arranged orthogonally to create a four-port UWB MIMO antenna. The structure of the resulting four-port UWB MIMO antenna with out stub is depicted in Figure 8. Simulation results of its S-parameters are presented in Figure 9. It is evident that the operational frequency range of the four-port antenna spans from 1.7 GHz to 14 GHz. Moreover, the isolation between antenna elements—specifically S12, S14, S23, and S34—is greater than 15.5 dB, while S13 and S24 exhibit isolation greater than 12.1 dB.

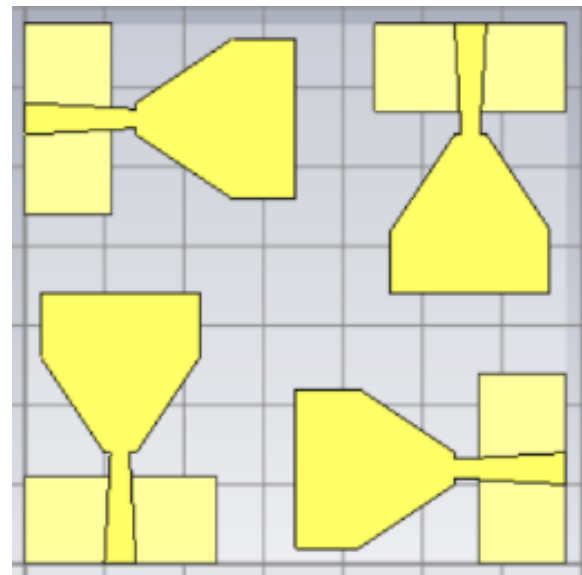
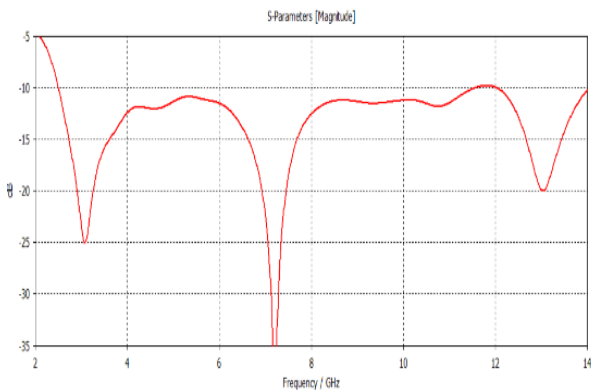


Fig 8. Schematic Diagram of Four Port UWB MIMO Antenna with out stubs.



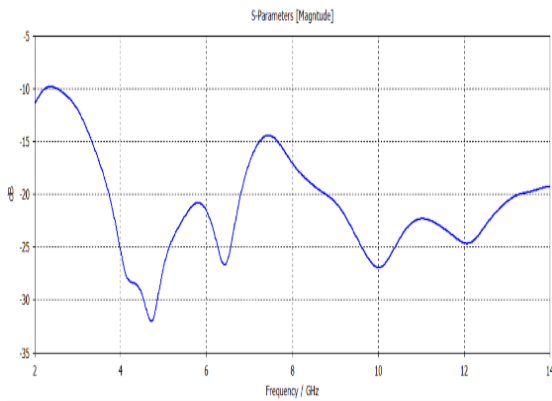
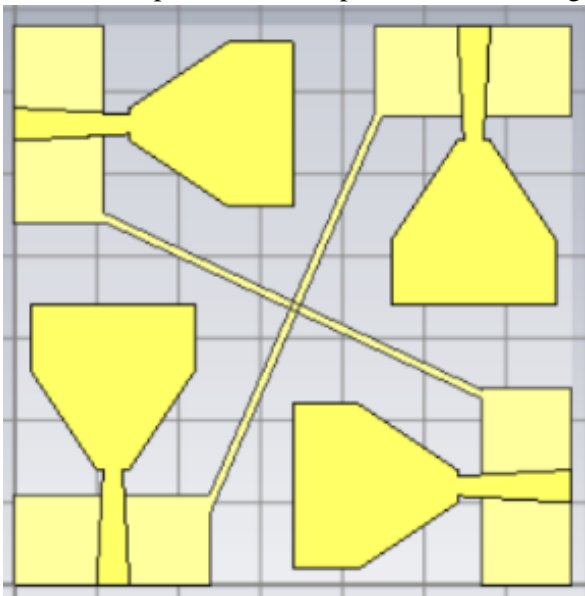


Fig 9.

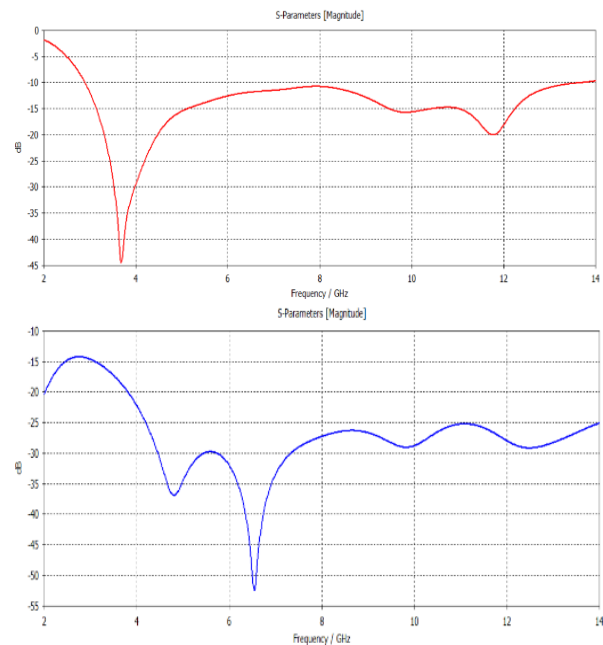
S11 and S21 Parameter waveforms.

6.DESIGN OF FOUR PORT UWB MIMO ANTENNA USING STUB

Similarly, a stub is inserted between the ground planes of two antenna elements positioned in opposite directions. This stub is connected to the ground planes, allowing the antennas to share a common ground plane. The structure of the resulting four-port UWB MIMO antenna with stub is depicted in Figure 10. Simulation results of its S-parameters are presented in the Figure



11. Fig 10. Schematic Diagram of Four Port UWB MIMO Antenna using Stubs.



Fig

11. S11 and S21 Parameter Waveforms.

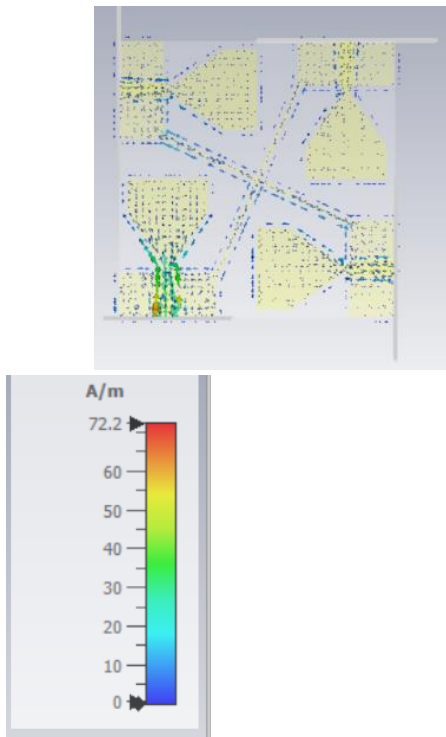


Fig 12. Surface Current distribution of four port antenna with stubs at $f=2\text{GHz}$.

Hence, the designed four-port antenna with stub maintains isolation exceeding 20.1 dB across the frequency range of 3.1 GHz to 10.6 GHz, demonstrating effective isolation between its antenna elements. This confirms that the utilization of stub connected to the ground plane of the four-port element achieves superior isolation in the design of the four-port antenna.

7.RESULTS

a)S-Parameters- In the design process of the Ultra-Wideband (UWB) Multiple-Input Multiple-Output (MIMO) antenna, this employs electromagnetic simulation software to simulate and refine the antenna structure. Due to the symmetry of the antenna elements, the performance of one element can be inferred from the performance of others. Therefore, only the S-parameters of the left element are provided. Figure 10 displays the physically fabricated design of the four-port UWB MIMO antenna and also showcases the measured S-parameter results. The antenna's operational frequency range, as measured, spans from 1.9 GHz to

14 GHz with isolation exceeding 20.1 dB across the entire frequency band, indicating outstanding isolation performance. The comparison between measurement and simulation results demonstrates close agreement. However, slight discrepancies may arise due to factors such as incomplete shielding in the measurement environment and electromagnetic interference from the surroundings.

b)Radiation Characteristics- Figure 13 depicts the radiation pattern of the four-port Ultra-Wideband (UWB) Multiple-Input Multiple-Output (MIMO) antenna from simulation. The radiation patterns are shown at specific frequency points: 2 GHz, 4 GHz and 14 GHz. Each figure in Figure 11, labeled (a) to (c), illustrates the radiation patterns in the xoz-plane (E-plane) and the yoz-plane (H-plane) for both co-polarization and cross-polarization. In the simulation setup, the left port of the antenna is linked to the excitation source, while the right port is connected to a $50\ \Omega$ load. Observing the figures, it's notable that the cross-polarization pattern of the xoz-plane maintains bidirectional radiation. Meanwhile, the co-polarization pattern of the yoz-plane exhibits consistent omnidirectional radiation characteristics. Although there are distortions in the shape of the co-polarization pattern on the xoz-plane and the cross-polarization pattern on the yoz-plane as the frequency increases, the antenna generally demonstrates improved omnidirectional radiation characteristics within the passband range .

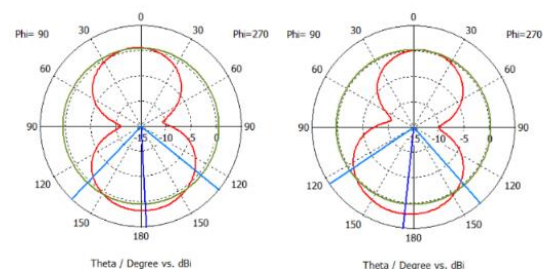


Fig13.a-Radiation patterns at 2 GHz

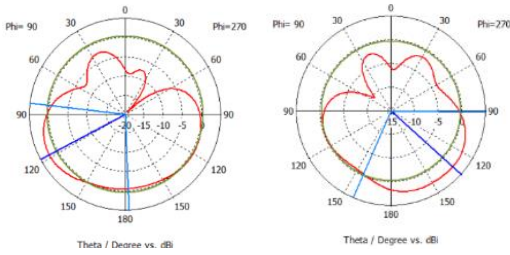
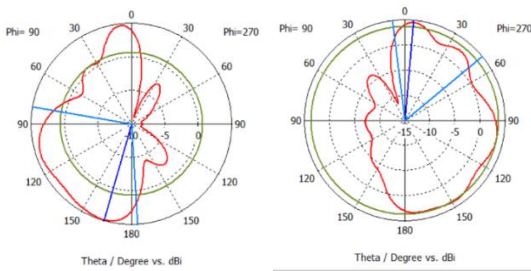


Fig 13.b-Radiation patterns at 8 GHz



13.c-Radiation patterns at 14 GHz.

The graph in Figure 14 displays the gain plots for a four-port antenna within the frequency range where the antenna operates effectively. This variation occurs due to discrepancies in the physical manufacturing process and external factors affecting the measurement environment. Notably, the maximum gain recorded during measurement falls short of the simulated

In MIMO (Multiple Input Multiple Output) antenna systems, maintaining a low envelope correlation coefficient (ECC) is crucial for optimal performance. Typically, the ECC should be of less than 0.5. The smaller the ECC, the greater the diversity gain, which can lead to significant improvements in signal quality, often up to around 10 dB. Figure 15 illustrates that across the entire frequency range where the antenna operates, the ECC remains consistently below 0.05. This value is substantially lower than the typical requirement for MIMO antennas, indicating exceptionally good performance. Essentially, this means that the antennas in the system exhibit minimal correlation between them, which is beneficial for achieving high-quality signal transmission and reception in diverse environments.

maximum gain, likely due to these errors and environmental interference.

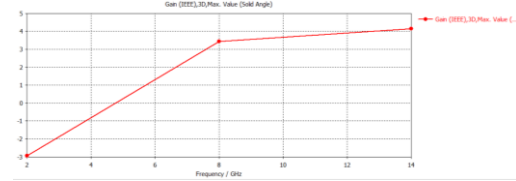
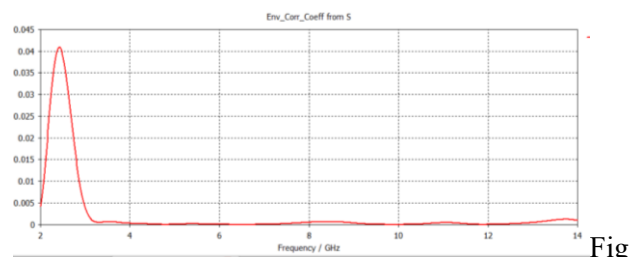


Fig 14. Gain graph (3D, Max Value, Solid Angle).

c) Diversity Characteristics-The performance of a Multiple Input Multiple Output (MIMO) antenna system relies heavily on the correlation between the channels formed by its transmitting and receiving ends. This correlation can be classified into two types: correlated and uncorrelated. The level of correlation significantly impacts the overall performance of the MIMO antenna. To better understand and discuss the correlation between antennas, a metric called the envelope correlation coefficient (ECC). This metric provides a clear depiction of the relationship between antennas in terms of their dependence on each other. The below equation uses far field data to calculate ECC and the ECC is used to calculate the diversity gain (DG).

$$P_c = \frac{\left| \int_0^{2\pi} \int_0^\pi (X_{PR} \cdot E_{\theta_i} \cdot E_{\theta_j}^* + P_{\theta} + E_{\phi_i} \cdot E_{\phi_j}^* \cdot P_{\phi}) d\Omega \right|^2}{\int_0^{2\pi} \int_0^\pi (X_{PR} \cdot E_{\theta_i} \cdot E_{\theta_i}^* + P_{\theta} + E_{\phi_i} \cdot E_{\phi_i}^* \cdot P_{\phi}) d\Omega \times \int_0^{2\pi} \int_0^\pi (X_{PR} \cdot E_{\theta_j} \cdot E_{\theta_j}^* + P_{\theta} + E_{\phi_j} \cdot E_{\phi_j}^* \cdot P_{\phi}) d\Omega}$$

$$DG = 10 \sqrt{1 - |P_c|^2}$$



15. Simulation and graph of ECC Results

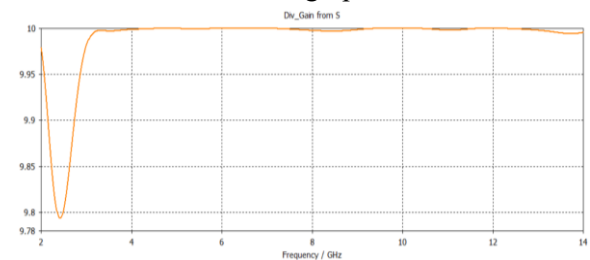


Fig 16. Simulation and graph of DG Results

The Mean Effective Gain (MEG) serves as a crucial metric for assessing the diversity performance of MIMO antennas. It provides insight into how effectively antenna elements can receive electromagnetic signals, especially in environments prone to multipath fading, where signals take multiple paths to reach the receiver. Figure 17 displays the measurement results of MEG. Both MEG 1 and MEG 2 hover around -3 dB within the operational frequency range. Additionally, the difference between the two remains within ± 3 dB. In simpler terms, the MEG results show that the antennas perform consistently well in receiving signals, even in challenging multipath fading conditions, which is essential for reliable communication.

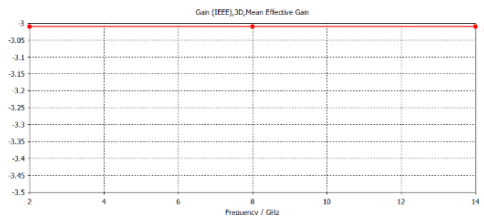


Fig 17. Graph of MEG Results

No of elements	Dimension (mm ²)	Operating band (GHz)	Isolation (dB)	Method	Gain (dBi)	ECC
2	50 × 40	2.43–12	>15	DGS	0.4–6	<0.016
2	24 × 30	3–12.6	>16.3	Stub	2–4.8	<0.05
2	35 × 35	3–12	>20			
4	50 × 50	3.1–10.6	>15	Diversity	—	<0.3
2	23 × 26	3.1–10.6	>20	DGS	2–4.5	<0.01
2	33 × 48	2–13.7	>20	Stub	1.1–4.3	<0.15
4	30 × 30	3–11	>20	EBG	2.5–6.8	<0.006
2	50 × 35	3–11	>25	DGS and stub	4–6.2	<0.004
4	38 × 38	3–20	>17	Diversity	1.3–6.2	<0.08
2	20 × 34	3.1–10.6	>20	DGS and stub	2–4	<0.2
1	18 × 12	3.7–14	>20.2			
2	18 × 28	1.9–14	>15.5	Stubs	0.4–4.8	<0.09

Fig

18. Performance comparison of proposed antenna with other reported antennas.

Our designed antenna is of 4 port with dimension 34×34(mm²) with in the operating band of 3.1 to 10.6(GHz) of high isolation > 20.1(dB) using stubs method with ECC <0.05. After conducting a detailed analysis of each antenna's performance as outlined in the table, it becomes evident that the MIMO antenna designed in this study offers several notable advantages. Firstly, it boasts a broader operational frequency band compared to previous designs. Additionally, it achieves higher isolation between antenna elements while still maintaining a compact and miniature structure.

Moreover, the antenna demonstrates superior gain characteristics, meaning it can effectively transmit and receive signals with improved efficiency. Furthermore, the envelope correlation coefficient (ECC) meets the specific application requirements, indicating that the antennas exhibit low correlation, which is desirable for MIMO systems. Considering these factors, the MIMO antenna developed in this research proves to be highly suitable for integration into miniaturized Ultra-Wideband (UWB) communication equipment. Its enhanced performance in terms of frequency coverage, isolation, gain, and ECC aligns well with the demands of modern communication systems that prioritize compactness and efficiency.

8. CONCLUSION

In our study, we developed a compact highly isolated Ultra-Wideband (UWB) Multiple Input Multiple Output (MIMO) antenna. We enhanced the isolation between antenna elements by incorporating stubs between the ground planes of the two elements. Additionally, we extended the design from a two-port MIMO antenna to a four-port (34 x 34 x 1.6 mm³) configuration while maintaining the same connection structure. To ensure effective grounding and isolation, we cross-connected the stubs between antenna elements positioned in opposite directions. Simulation results demonstrate that the four-port antenna achieves impressive isolation, exceeding 20.1 dB, across a wide operating frequency range of 3.1–10.6 GHz. Furthermore, measurements confirmed that the isolation remains consistently above 20.1 dB within the specified frequency band, with an envelope correlation coefficient (ECC) below 0.05, indicating minimal correlation between antenna elements. Additionally, the Mean Effective Gain (MEG) and Coupling Correlation Level (CCL) measurements indicate strong MIMO antenna performance.

In summary, our UWB MIMO antenna exhibits excellent UWB performance, exceptional isolation and is well-suited for integration into UWB wireless communication systems offering improved signal transmission and reception capabilities

9. REFERENCES

- [1] W. M. Saadh, K. Ashwath, P. Ramaswamy, T. Ali, and J. Anguera, "A uniquely shaped MIMO antenna on FR4 material to enhance isolation and bandwidth for wireless applications," *AEU-International Journal of Electronics and Communications*, vol. 123, Article ID 153316, 2020.
- [2] M. Irshad Khan, M. I. Khattak, S. U. Rahman, A. B. Qazi, A. A. Telba, and A. Sebak, "Design and investigation of modern UWB-MIMO antenna with optimized isolation," *Micromachines*, vol. 11, no. 4, p. 432, 2020.
- [3] Y. Sharma, D. Sarkar, K. Saurav, and K. V. Srivastava, "Three element MIMO antenna system with pattern and polarization diversity for WLAN applications," *IEEE Antennas and Wireless Propagation Letters*, vol. 16, pp. 1163–1166, 2017.
- [4] L. Wang, Z. Du, H. Yang et al., "Compact UWB MIMO antenna with high isolation using fence-type decoupling structure," *IEEE Antennas and Wireless Propagation Letters*, vol. 18, no. 8, pp. 1641–1645, 2019.
- [5] B. Yang, M. Chen, and L. Li, "Design of a four-element WLAN/LTE/UWB MIMO antenna using half-slot structure," *AEU—International Journal of Electronics and Communications*, vol. 93, pp. 354–359, 2018.
- [6] T. Addepalli and V. R. Anitha, "A very compact and closely spaced circular shaped UWB MIMO antenna with improved isolation," *AEU - International Journal of Electronics and Communications*, vol. 114, Article ID 153016, 2020.
- [7] A. Altaf, A. Iqbal, A. Smida et al., "Isolation improvement in UWB-MIMO antenna system using slotted stub," *Electronics*, vol. 9, no. 10, p. 1582, 2020.
- [8] W. A. E. Ali and A. A. Ibrahim, "A compact double-sided MIMO antenna with an improved isolation for UWB applications," *AEU—International Journal of Electronics and Communications*, vol. 82, pp. 7–13, 2017.
- [9] L. Wang, Z. Du, H. Yang et al., "Compact UWB MIMO antenna with high isolation using fence-type decoupling structure," *IEEE Antennas and Wireless Propagation Letters*, vol. 18, no. 8, pp. 1641–1645, 2019.
- [10] R. Chandel, A. K. Gautam, and K. Rambabu, "Tapered fed compact UWB MIMO-diversity antenna with dual bandnotched characteristics," *IEEE Transactions on Antennas and Propagation*, vol. 66, no. 4, pp. 1677–1684, 2018.
- [11] A. Kumar, A. Q. Ansari, B. K. Kanaujia, and J. Kishor, "High isolation compact four-port MIMO antenna loaded with CSRR for multiband applications," *Frequenz*, vol. 72, no. 9-10, pp. 415–427, 2018.
- [12] J. Prasanth Kumar and G. Karunakar, "Compact UWB MIMO triple notched antenna for isolation reduction," *Wireless Personal Communications*, vol. 115, no. 3, pp. 2113–2125, 2020.